PUBLICATIONS OF THE ASTRONOMICAL SOCIETY OF THE PACIFIC, **120**:425–429, 2008 April

The Temperature Dependence of the Pointing Model of the Hamburg Robotic Telescope

M. MITTAG,[1] A. HEMPELMANN,[1] J. N. GONZALEZ-PEREZ,[1] AND J. H. M. M. SCHMITT[1]

Received 2007 December 17; accepted 2008 January 23; published 2008 March 31

ABSTRACT. A first pointing model was determined during commissioning of the Hamburg Robotic Telescope in 2005 September. Pointing accuracy better than 3″ was achieved with this model in those days. However, in the course of the rest of 2005, a systematic increase of the telescope mispointing mainly in azimuth was observed having been suggested a strong dependence on ambient air temperature. We therefore checked this relation between temperature and pointing accuracy by systematic observations targeted on temperature. We made 16 pointing-model estimates during the year 2006 and correlated the model parameters with temperature. While most of the parameters are either not correlated or merely weakly correlated with temperature we find a clear temperature dependence of a misalignment of the optical axis with the telescope tube. We suggest that the M3 mounting is responsible for this.

1. INTRODUCTION

Long-term spectroscopic monitoring of, for example, stellar activity cycles as observed in Ca II H and K, is one of the science areas where small telescopes can provide extremely valuable contributions. The best performance in terms of cost efficiency is provided by fully robotic telescopes. The Hamburg Robotic Telescope (HRT) is such a fully robotic spectroscopic telescope. The HRT was built by the company Halfmann Teleskoptechnik GmbH (Germany) and delivered to the Hamburg Observatory in 2005. The HRT is a 1.2 m aperture Cassegrain-Nasmyth $F/8$-type telescope with Zeiss three mirror optics made of Schott Zerodur glass ceramics. The HRT has an altitude-azimuth (alt-az) mounting, final direct drives with high-precision absolute encoders, a hydraulic bearing in azimuth and a roller bearing in elevation. The parabolic M1 mirror is actively supported with 18 axial and 12 radial levers. The instrumental platform is mounted at a field of view derotator in one Nasmyth focus, located approximately 50 cm behind the derotator flange. This platform contains the acquisition and guiding unit, a fiber entrance unit, and a calibration lamps unit. The fiber entrance unit feeds the telescope beam into a fused silica fiber, which connects the telescope with a spectrograph. The size of fiber on the sky is ~3″ for a 100 μm fiber with a pinhole of 160 μm aperture that is mounted in front of the entrance microlens of the fiber. The microlens matches the $F/8$ telescope beam to the $F/4.5$ collimator beam of the spectrograph. The Heidelberg Extended Range Optical Spectrograph (HEROS) is of type *Échelle*, covering a free spectral range 345–865 nm in two channels with a spectral resolution of approximately 20,000.[2]

The HRT will be operated fully automatically. The robotic software and some non-telescope hardware components are presently under construction, and first spectroscopic light was achieved in 2007 October. The telescope's performance is currently being studied at Hamburg, where the average seeing was found to be about 2.8″. Under those conditions short-time tracking fluctuations actually result from seeing limitations rather from the telescope. Clearly, a crucial element for the overall performance of the HRT is the ability of the system to keep the target star on the fiber fed into the spectrograph. While the HRT autoguiding system is supposed to ensure an optimal placement of the target star on the fiber, the telescope's pointing and tracking accuracy are also very important, because the duty cycle of the autoguider, in combination with tracking errors, can generate system oscillations with ensuing negative effects on image quality and light loss at the fiber. Therefore, despite the presence of the autoguiding system, good tracking and, hence, a good pointing model are essential for an optimal system performance.

For these reasons extensive studies of the HRT pointing model have been carried out. A first pointing model was determined during commissioning in 2005 September at the average temperature of 17° C. During that time the temperature was steady and warm and the pointing model was stable with typical mispointings of the order of 1–3″, well below the specified value for the pointing accuracy of the telescope (Δaz,Δel $< 5''$). In the course of the season a systematic trend of mispointing

[1] Universitaet Hamburg, Hamburger Sternwarte, Gojenbergsweg 112, 21029 Hamburg, Germany; mmittag@hs.uni-hamburg.de; ahempelmann@hs.uni-hamburg.de; jgonzalezperez@hs.uni-hamburg.de; jschmitt@hs.uni-hamburg.de

[2] The reader can find a more detailed description of the HRT project at the HRT Web page: www.hs.uni-hamburg.de/DE/Ins/Per/Hempelmann/HRT/index.html.

mainly in the azimuth direction was observed leading to the suggestion that the pointing model might be temperature dependent. Therefore extensive studies of the pointing and tracking accuracy of the telescope were carried out between autumn 2005 and summer 2006, which showed that the pointing model does indeed depend on temperature and that the pointing and tracking performance can be considerably improved by the explicit inclusion of temperature in the pointing model.

2. THE POINTING MODEL

The pointing model describes the discrepancy between the theoretical and the actual position of the telescope. The determination of the theoretical position includes all "natural" or astronomical effects such as precession, nutation, stellar proper motion, refraction, aberration, and the divergence between UTC and UT1. The mismatch between theoretical and actual pointing position is due to technical reasons such as, for example, misalignment errors (for details see below; see also Plaza 2001; Zheng et al. 2004; Zhang & Wu 2001).

The pointing model of the HRT is based on a classical physical pointing model in the form described by Plaza (2001). The physical model, unlike the empirical one (e.g., a series of spherical harmonics), has the advantage that it gives information about the structure of the telescope, and the reason for a change in the parameters can be easily traced back (Maddalena 1994). The classic pointing model was modified by the Halfmann company to include an encoder effect, and later, after a precommissioning test phase before 2005, further HRT-specific empirical components were introduced by A. Hempelmann and J. N. Gonzalez-Perez. The currently used pointing model of the HRT is described by equations (1) and (2) for the azimuth and elevation corrections:

$$\begin{aligned}\Delta\mathrm{az}\cdot\cos(\mathrm{el}) = {} & -\mathrm{BNP} + \mathrm{AN_A}\cdot\sin(\mathrm{az})\cdot\sin(\mathrm{el}) \\ & - \mathrm{AE_A}\cdot\cos(\mathrm{az})\cdot\sin(\mathrm{el}) + \mathrm{NPAE}\cdot\sin(\mathrm{el}) \\ & + \mathrm{AOFF}\cdot\cos(\mathrm{el}) + \mathrm{AES}\cdot\sin(\mathrm{az})\cdot\cos(\mathrm{el}) \\ & + \mathrm{AEC}\cdot\cos(\mathrm{az})\cdot\cos(\mathrm{el}), \end{aligned} \quad (1)$$

$$\begin{aligned}\Delta\mathrm{el} = {} & \mathrm{EOFF} + \mathrm{AN_E}\cdot\cos(\mathrm{az}) + \mathrm{AE_E}\cdot\sin(\mathrm{az}) \\ & + \mathrm{EES}\cdot\sin(\mathrm{el}) + \mathrm{EEC}\cdot\cos(\mathrm{el}) + \mathrm{C1}\cdot\sin(2\cdot\mathrm{az}) \\ & + \mathrm{C2}\cdot\cos(2\cdot\mathrm{az}) + \mathrm{C3}\cdot\sin(3\cdot\mathrm{az}) \\ & + \mathrm{C4}\cdot\cos(3\cdot\mathrm{az}) + \frac{\mathrm{C5}}{\cos(\mathrm{el})} \end{aligned} \quad (2)$$

In equations (1) and (2) the parameter AN is a tilt of the azimuth axis to the north and AE is a tilt to east; the subscript A denotes the azimuth correction and E the elevation correction. These quantities are physically the same for the azimuth and elevation equations but have been given different symbols in the two equations because they can be evaluated from either equation (1)) or equation (2)). Thus, both equations are coupled in general. However, a better pointing behavior was observed with decoupled equations for the pointing model of the HRT, leading to slightly different values of AN and AE in both equations.

The parameter NPAE is the deviation of the elevation axis from horizontal, and BNP is a misalignment of the optical axis to the telescope tube axis. AOFF and EOFF are the zero-point offsets of the encoders in azimuth and elevation, respectively. The parameters AES, EES, AEC, and EEC describe an elliptical encoder deformation and/or a miscentering of the encoders. Furthermore, EEC has a contribution of the flexure of the telescope tube under gravity. C1 to C5 are empirical HRT specific parameters. The C1 to C4 describe two observed waves in elevation where the wave elongation depends on azimuth (a 180° and a 120° wave, respectively). These four terms could represent irregularities in the bearing race (Stark et al. 2001; Condon 1992). C5 is an empirical parameter introduced to correct a mispointing in elevation observed only near the zenith, the physical reason of which has not yet been identified.

3. POINTING MEASUREMENTS AND MODEL CALCULATIONS

3.1. Measurements

For this study, a simplified instrument was installed, consisting only of a SBIG-ST7 acquisition and guiding CCD camera (pixel size $\sim 0.2''$, field of view $\sim 2.5 \times 1.7'$), which was mounted directly at the Nasmyth focus. During the observations, the derotator was switched off and the target star was centered at the position of the derotator axis. Without derotator, the transformation between the x/y CCD coordinate system and the alt-az coordinate system is a rotation, the angle of which is simply the elevation. During 16 nights between 2006 March 13 and 2006 June 13, with temperatures ranging from -6.4°C to 25.8° C, we took measurements of the mispointing of the telescope at different positions of the sky in order to determine the pointing-model parameters.

The determination of a good pointing model requires data uniformly distributed over the sky. A total of 180 sky positions (azimuth and elevation) served as a basis for an individual model. These positions were selected by the astronomer and listed in a code for a robotic selection of an appropriate target star from the HIPPARCOS Input Catalogue. Then the catalog position was sent to the telescope, which slews and tracks the telescope to this reference position. An automatic acquisition of the star delivers the offsets Δaz and Δel at the encoders. Finally, the azimuth offset must be corrected for elevation [multiplication with cos(el)] to find the offset at the sky position. These offsets together with the actual position of the telescope are the input for the parameter calculations. The whole automatic procedure lasts approximately 4 hr. Sixteen model determinations were therefore carried out and used as a basis for this investigation.

3.2. Calculations

The pointing-model parameters are determined using least squares. We used the standard deviation of the residuals of the initial fits as σ for each data point, allowing us to attach errors to the parameters calculated from the fits.

The mean standard deviation of the residuals was for azimuth $(2.4 \pm 0.4)''$ and for elevation $(1.5 \pm 0.1)''$. The higher value in azimuth results from hitherto undiscovered waves in the azimuth offsets, whose nature is the same as the C1–C4 terms in equation (2) (Mittag 2006). The parameter errors are estimated via the information matrix

$$\alpha_{\mathrm{kl}} = \sum_{i=1}^{n} \frac{1}{\sigma^2} \left[\frac{\partial y(x_i; a)}{\partial a_{\mathrm{k}}} \frac{\partial y(x_i; a)}{\partial a_{\mathrm{l}}} \right] \tag{3}$$

and the covariance matrix

$$\mathbf{C} \equiv \alpha_{\mathrm{kl}}^{-1}. \tag{4}$$

The 1 σ error of the parameter is (Press et al. 1986)

$$\sigma_{\mathrm{parameter}} \equiv \sqrt{C_{ii}}. \tag{5}$$

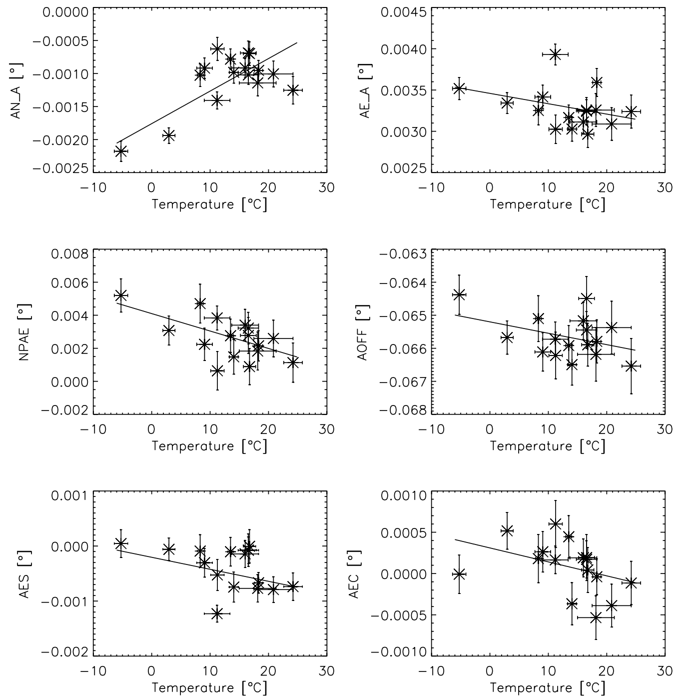

FIG. 2.—Relation between the parameters of the pointing model in azimuth and temperature.

4. RESULTS

We plot the parameters of the pointing model versus the air temperature during our measurements in Figures 1–3. The figures show some clear correlations between the temperature and the respective parameters; note that we assume parameter C5 to be constant because its value is very small and a temperature trend is not visible in Figure 3. Some parameters show quite strong scattering, which is partly due to the high mutual correlation observed between some parameters (Mittag 2006). For example, the correlation coefficient between the parameters NPAE and AOFF is typically 0.95. Most of the correlations result from the fact that equations (1) and (2) contain elevation dependent 360° waves, which are covered with data points only in a small interval between el $= 20°$ and el $= 90°$.

The temperature trends were calculated with the IDL POLY_FIT routine using the parameter errors as measurement errors. In the next step, we checked for the probability of a correlation between the parameters and the temperature. We used the t-Student test, which is a test used to determine the independence between two samples. From the correlation coefficient the t value can be estimated as shown in equation (6) (Bronstein et al. 2001); this value has approximately a t-Student distribution with a number of degrees of freedom equal to $n - 2$, where n is the number of measurements:

$$t = \frac{r\sqrt{n-2}}{\sqrt{1-r^2}}. \tag{6}$$

The value of t_{cutoff}, for which we can consider the existence of a significant correlation between the parameter and the temperature is ≥ 3.79 for a significance level $\geq 99.9\%$ (Bronstein et al. 2001). Our analyses are summarized in Table 1, where we show the coefficients of the linear relations between the parameters and the temperature. The absolute values of the correlation coefficient (r) and the parameter t are also given.

The correlation coefficient and the absolute values of t shown by BNP, EOFF, EES, EEC and C2 are clearly higher than the t_{cutoff} at 99.9%. For these parameters there exist clear correlations between the parameter and temperature. The largest effects are observed for BNP (see Fig. 1). BNP is a constant in equation (1). Hence, the observed systematic shift of the mispointing mainly in azimuth during autumn 2005 is explained by a systematic trend in the misalignment of the optical axis with the tube. For parameters with $2.62 \leq t < 3.79$ a possible correlation with the temperature is suspected and we will monitor its behavior in the future, while for the parameters whose t value is

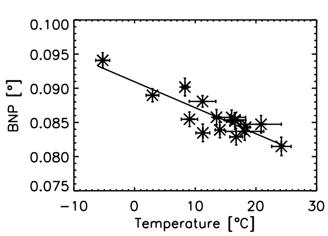

FIG. 1.—Parameter BNP vs. Temperature.

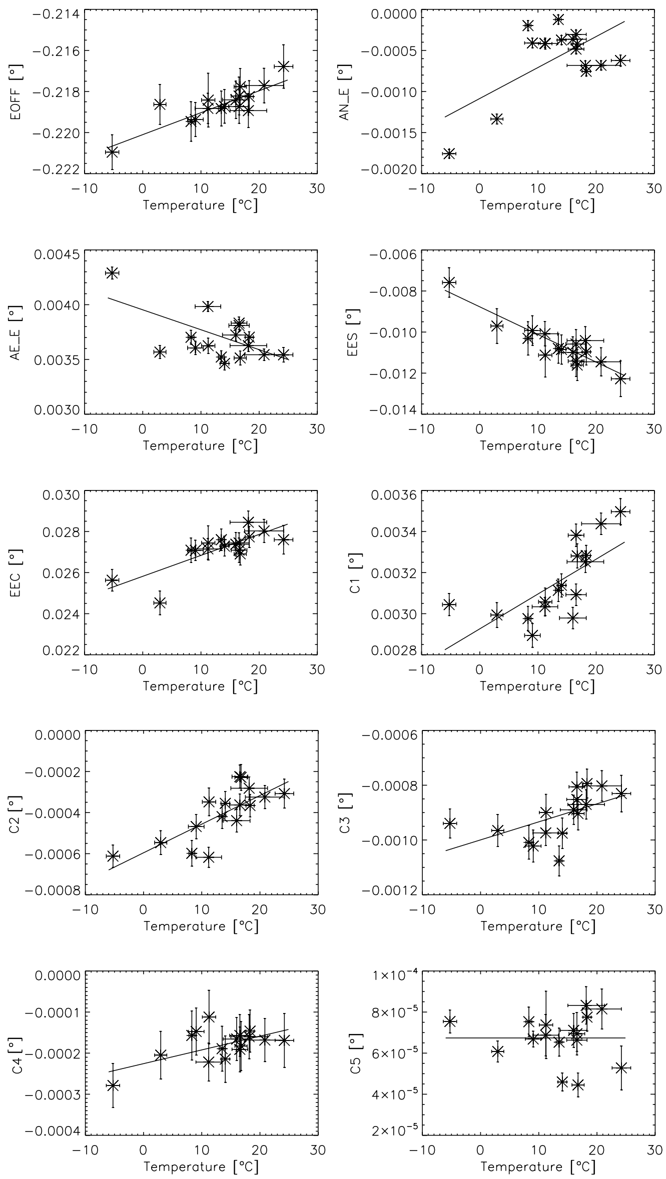

FIG. 3.—Relation between the parameters of the pointing model in elevation and temperature.

TABLE 1

THE LINEAR RELATIONS a + bT (°C) BETWEEN THE PARAMETERS OF THE POINTING MODEL AND THE AMBIENT AIR TEMPERATURE. IN ADDITION, THE CORRELATION COEFFICIENT (r) AND THE t-STUDENT VALUE (t) ARE SHOWN.

Parameter	a	b	$\|r\|$	$\|t\|$
BNP	0.0909 ± 0.0006	$-38.0 \times 10^{-5} \pm 4.1 \times 10^{-5}$	0.88	6.77
AN_A	-0.00176 ± 0.00008	$4.9 \times 10^{-5} \pm 0.6 \times 10^{-5}$	0.66	3.28
AE_A	0.00346 ± 0.00008	$-1.3 \times 10^{-5} \pm 0.5 \times 10^{-5}$	0.33	1.31
NPAE	0.0041 ± 0.0005	$-10.6 \times 10^{-5} \pm 3.7 \times 10^{-5}$	0.61	2.88
AOFF	-0.0652 ± 0.0003	$-3.4 \times 10^{-5} \pm 2.3 \times 10^{-5}$	0.43	1.79
AES	-0.0002 ± 0.0001	$-2.2 \times 10^{-5} \pm 0.9 \times 10^{-5}$	0.42	1.75
AEC	0.0003 ± 0.0001	$-1.7 \times 10^{-5} \pm 0.9 \times 10^{-5}$	0.41	1.68
EOFF	-0.2201 ± 0.0005	$10.7 \times 10^{-5} \pm 3.2 \times 10^{-5}$	0.85	6.02
AN_E	-0.00108 ± 0.00003	$3.8 \times 10^{-5} \pm 0.2 \times 10^{-5}$	0.58	2.69
AE_E	0.00395 ± 0.00003	$-1.8 \times 10^{-5} \pm 0.2 \times 10^{-5}$	0.57	2.59
EES	-0.0087 ± 0.0004	$-13.5 \times 10^{-5} \pm 2.7 \times 10^{-5}$	0.91	8.10
EEC	0.0258 ± 0.0003	$10.2 \times 10^{-5} \pm 2.0 \times 10^{-5}$	0.78	4.63
C1	0.00293 ± 0.00003	$1.7 \times 10^{-5} \pm 0.2 \times 10^{-5}$	0.70	3.70
C2	-0.00060 ± 0.00003	$1.4 \times 10^{-5} \pm 0.2 \times 10^{-5}$	0.76	4.35
C3	-0.00100 ± 0.00003	$0.7 \times 10^{-5} \pm 0.2 \times 10^{-5}$	0.56	2.55
C4	-0.00023 ± 0.00003	$0.3 \times 10^{-5} \pm 0.2 \times 10^{-5}$	0.56	2.51
C5	$6.7 \times 10^{-5} \pm 0.3 \times 10^{-5}$	…	0.11	0.43

below 2.62 ($<99\%$), the correlation is not clear and, hence, a (possible) temperature dependence cannot be regarded as significant.

How does the temperature dependence of the pointing-model parameters reflect itself in the actual performance of the telescope? In order to demonstrate this we consider the pointing performance at an azimuth and elevation location of both 40° measured at different temperatures. Figures 4*a* and 4*b* show the azimuth and elevation offsets. We observe a min-max scatter of 40″ in azimuth and 10″ in elevation when the temperature effect is not eliminated (Fig. 4*a*). We then computed the azimuth and elevation offsets with a temperature-dependent pointing model with parameters as provided in Table 1 and show the resulting azimuth offset ("residuals") versus elevation offset scatter plot in Figure 4*b*. The reduction in scatter between Figures 4*a* and 4*b* is obvious; thus, the inclusion of temperature leads to a significant pointing improvement.

5. CONCLUSION

Our analysis clearly shows that the pointing model of the HRT does not only depend on target coordinates but also on temperature. One possible technical reason for this temperature dependence is the thermal expansion of the metal. We find the strongest dependence for the parameter BNP, which changes by 41″ in the temperature range from $-5°$ C to 25° C. The reason is a possible thermal expansion of the mounting of the M3 mirror. For example, through the thermal expansion of the mirror mounting, the tilting angle (initially 45°) changes, which leads to a tipping of the optical axis. With a typical coefficient of expansion for steel of $11.1\ \mu\mathrm{m\,m^{-1}\,K^{-1}}$ at 20° C and a possible maximum distance between the supports of the M3 holder of 0.350 m (the actual value is smaller but not precisely known), one obtains a change in BNP of 69″. This is an upper limit and is indeed larger than the value of our measurement.

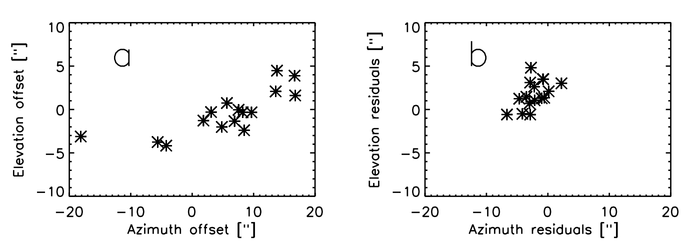

FIG. 4.—Azimuth offset vs. elevation offset; (*a*) without correction of the temperature effect; (*b*) after elimination of the temperature effect.

Unfortunately we have only two measurements below 5° C. Without these two data points the trends with temperature for some parameters are changed, as for example AN_A. However, in other cases (e.g., BNP and EOFF) there are no changes in the trends. Another problem is that the air temperature is usually not constant during the pointing measurements which last about four hours. Clearly, this does effect the derived parameter accuracy.

In summary, we conclude that—depending of the design of a telescope and its construction materials—the ambient temperature can have an important influence on the telescope pointing. However, the principal deterministic behavior of the temperature dependence allows a remarkable improvement of the pointing behavior via software whenever an initial pointing-model determination has been obtained. Our tests after the implementation of a temperature-dependent pointing model yielded stability of the pointing accuracy within our 5″ limit to date, which then also significantly improved the tracking accuracy.

REFERENCES

Bronstein, I. N., Semendjajew, K. A., Musiol, G., & Mühlig, H. 2001, Taschenbuch der Mathematik (5th ed.; Frankfurt am Main: Verlag Harri Deutsch)

Condon, J. J. 1992, GBT Pointing Equations, GBT Tech. Memo. GBT75

Maddalena, R. J. 1994, Refraction, Weather Station Components, and Other Details for Pointing the GBT, GBT Tech. Memo. 112

Mittag, M. 2006, Diploma thesis, Univ. Hamburg

Plaza, D. 2001, Diploma thesis, Univ. Tübingen

Press, W. H., Flannery, B. P., Teukolsy, S. A., & Vertterling, W. T. 1986, Numerical Recipes (Cambridge, UK: Cambridge Univ. Press

Stark, A. A., Bally, J., Balm, & S. P., et al. 2001, PASP, 113, 567

Zhang, X., & Wu, L. 2001, Chinese Astron. Astrophys., 25, 499

Zheng, X., Wang, W., Zhang, Y., & Feng, H. 2004, Chinese Astron. Astrophys., 28, 105